

Incoherent transport through molecules on silicon in the vicinity of a dangling bond

Hassan Raza

NSF Network for Computational Nanotechnology and School of Electrical and Computer Engineering, Purdue University, West Lafayette, Indiana 47907, USA

School of Electrical and Computer Engineering, Cornell University, Ithaca, New York 14853, USA

Kirk H. Bevan and Diego Kienle

NSF Network for Computational Nanotechnology and School of Electrical and Computer Engineering, Purdue University, West Lafayette, Indiana 47907, USA

(Received 28 November 2007; published 25 January 2008)

We theoretically study the effect of a localized unpaired dangling bond (DB) on occupied molecular orbital conduction through a styrene molecule bonded to a n^{++} H:Si(001)-(2×1) surface. For molecules relatively far from the DB, we find good agreement with the reported experiment using a model that accounts for the electrostatic contribution of the DB provided we include some dephasing due to low lying phonon modes. However, for molecules within 10 Å to the DB, we have to include electronic contribution as well along with higher dephasing to explain the transport features.

DOI: 10.1103/PhysRevB.77.035432

PACS number(s): 85.65.+h, 73.20.-r, 73.63.-b

I. INTRODUCTION

Interest in atomic scale conduction continues to grow at a rapid pace in both the engineering and scientific communities. The comparatively stable C-Si bond and the well characterized Si surface chemistry^{1,2} not only place organic molecules in an ideal position to complement existing Si technology but also offer a unique platform to study scientific phenomena^{3,4} with experimental reproducibility. Notably, Si contacts may give rise to novel features such as negative differential resistance,⁵⁻⁷ although the mechanism is not yet established.⁸

In Si technology, dangling bond (DB) defects in the form of P_b centers have created reliability issues—consider negative bias temperature instability in metal-oxide-Si structures. However, one could engineer such defects to be useful in novel devices. Recently, Piva *et al.*⁹ observed significant shifts in the onset voltages along a styrene chain as a function of distance from a negatively charged unpaired DB on a n^{++} H:Si(001)-(2×1) surface using scanning tunneling spectroscopy (STS). In this paper, we theoretically study their results. A comparison between calculated and experimentally observed current-voltage (I - V) plots is shown in Fig. 1. The DB, being negatively charged, pushes molecular levels upward. A schematic energy level and/or band diagram is shown in Fig. 1. The onset voltage depends on the gap between the equilibrium chemical potential (μ_0) and molecular levels. Given that the onset voltage is decreasing in the vicinity of the DB, one concludes that conduction is through occupied orbitals. The trend would have been reversed for unoccupied orbital conduction.

Furthermore, observed onset voltages for molecules 4 and 8 Å (Ref. 10) away from the DB are grouped together; whereas a molecule 12 Å away has a distinctly different onset voltage. Electrostatically, one would expect them to follow an inverse distance relationship. To explain the above discrepancy, we propose that the DB also affects the I - V characteristics of the styrene chain electronically by intro-

ducing a near-midgap state in the local density of states (LDOS) of Si atoms 4 and 8 Å away. For these molecules, this contribution would lead to an early onset of conduction at approximately 0.5 V (rather than 1.2 V due to the bulk Si band gap), as shown in Fig. 1. Since the DB wave function decays exponentially, this contribution would be nearly absent for a molecule 12 Å away. Apart from this, the effect on

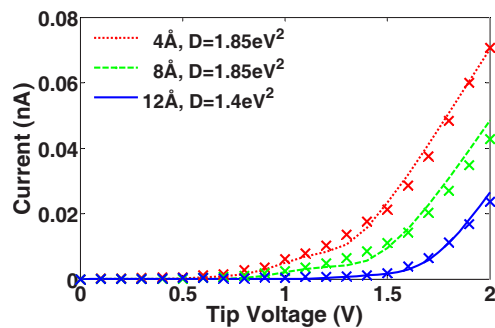
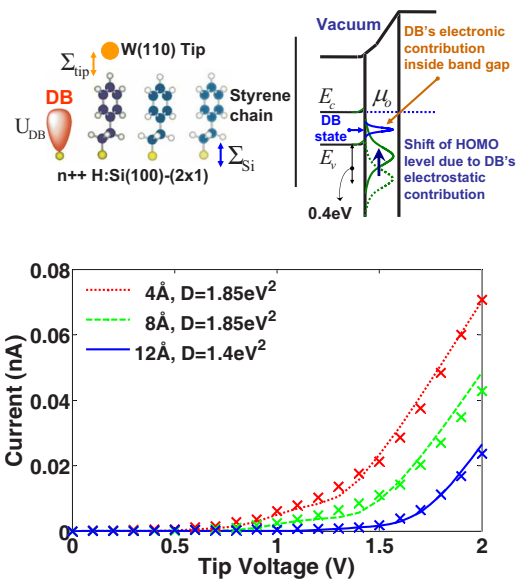


FIG. 1. (Color online) Calculated transport properties of a styrene molecule bonded to a n^{++} H:Si(001)-(2×1) surface in the vicinity of a negatively charged DB. Experimental data are indicated by × marks (Refs. 9 and 10). As a function of decreasing distance from the DB, the onset voltages shift toward lower tip voltages implying occupied molecular orbital conduction. I - V plots for molecules 4 and 8 Å away have grouped onset voltages. The electrostatic and electronic contributions of the DB are included in these calculations. We assume a lower dephasing strength (D) of 1.4 eV² for the molecule that is farthest from the DB, as compared to 1.85 eV² for the closer ones.

transport due to the DB state would be pronounced when the highest occupied molecular orbital (HOMO) level is sufficiently broadened to form a significant overlap with the DB state, as shown in the inset of Fig. 2. Moreover, this effect would be diminished if the HOMO level is too far from the DB state.

The impact of dephasing due to low lying phonons on experimentally observed line shapes is further explored in this paper. In molecular junctions, the dominant phonon modes are the ones having low energy, which arise due to the combined motion (translational, rotational, etc.) of the entire molecule relative to the contacts and have been discussed theoretically in Refs. 11 and 12. Experimentally, some evidence of the presence of these low lying modes is available.^{13–15} Since experimental results are suggestive, a detailed study needs to be done to establish it on a solid footing. These low lying phonon modes are excited due to inelastic electron-phonon scattering. Similarly, the styrene should be able to vibrate, rotate, and move with respect to the Si and tip contacts and, hence, we expect a similar trend. Since $\hbar\omega \ll k_B T$ at room temperature for these modes, we include their effect through elastic dephasing for simplicity. Furthermore, broadening due to such modes could be large, as in Ref. 16. The dephasing strength used in our calculation gives a comparable broadening.

II. THEORETICAL MODEL AND ASSUMPTIONS

We use the single particle nonequilibrium Green's function formalism in the mean field approximation using a non-orthogonal basis to model quantum transport, as in Ref. 17. We extend this work by including elastic dephasing within the self-consistent Born approximation.^{18,19} The time-retarded Green's function is defined as

$$G = [(E + i0^+)S - H_d - U_d - U_{DB} - \Sigma_{Si,tip} - \Sigma_s]^{-1}, \quad (1)$$

where H_d is the device Hamiltonian and S is the overlap matrix. U_d is the potential experienced by the molecule and consists of (1) the Laplace potential due to the applied tip voltage, (2) the band lineup potential due to the Fermi level mismatch of n^{++} Si and tip contacts, and (3) Hartree and image potentials due to nonequilibrium statistics of the electrons on the molecular region. U_{DB} is the potential due to the negative charge on the unpaired dangling bond, which causes a shift in the molecular levels. The electrostatic and electronic boundary conditions are set by the tip voltage and contact self-energies ($\Sigma_{Si,tip}$), respectively. Σ_s is the scattering self-energy. In a nonorthogonal basis for the elastic dephasing, the scattering broadening function is given as²⁰

$$\Gamma_s(E) = \Sigma_s^{in} + \Sigma_s^{out} \approx DSA(E)S, \quad (2)$$

where Σ_s^{in} is the scattering inflow function and Σ_s^{out} is the scattering outflow function. D is the dephasing strength, which is a fourth rank tensor, but in our calculations, it is approximated by a scalar and is used as a fitting parameter. Treating D as a scalar would ignore the minute details of dephasing that may be otherwise present when a carrier gets scattered from one electronic state to another electronic state more strongly or weakly. A is the spectral function defined as

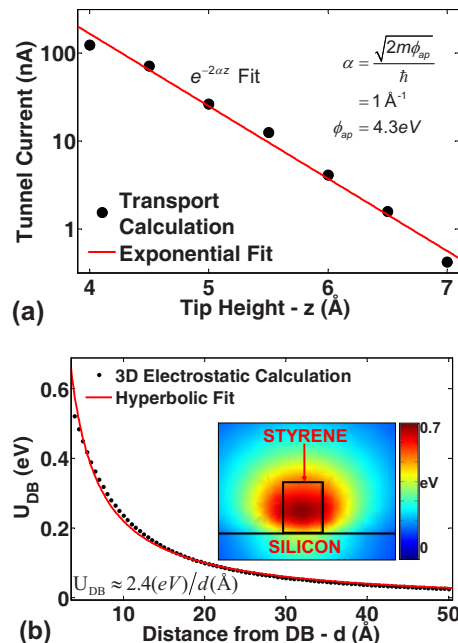


FIG. 2. (Color online) Tip modeling and electrostatic contribution of the DB. (a) Tunnel current as a function of tip height showing exponential decay, which gives an apparent barrier height of 4.3 eV. (b) A 3D continuum finite-element electrostatic calculation showing a hyperbolic trend in the average potential due to a negatively charged DB along a styrene chain. The insets show a contour plot potential profile 4 Å away.

$i(G - G^\dagger) = G^n + G^p$, where G^n and G^p are the electron and hole correlation functions, respectively. Using Eq. (2), the scattering self-energy is given as

$$\Sigma_s(E) = \frac{1}{\pi} \int_{-\infty}^{\infty} dy \frac{-\Gamma_s(y)/2}{E - y} - i \frac{\Gamma_s(E)}{2}. \quad (3)$$

It has been shown²¹ that the real part of $\Sigma_s(E)$ [calculated by the Hilbert transform as shown in Eq. (2)] is about a few meV for different organic molecules contacted by Au(111) electrodes due to slowly varying $\Gamma_s(E)$. We expect it to be small for the molecular transport through Si valence band due to the slowly varying density of valence band states. However, this approximation may not be appropriate for a one-dimensional contact such as a carbon nanotube or graphene nanoribbon due to van Hove singularities. Given that this calculation is computationally very expensive and has small effect on the final results, we ignore the real part of $\Sigma_s(E)$. Since Σ_s , G , $G^n(= -iG^<)$, and $\Sigma_s^{in}(= -i\Sigma_s^<)$ depend on each other, we solve for the above four quantities self-consistently along with the Hartree self-consistent loop of the applied tip voltage.

The electronic structure of Si(001),²² styrene,²³ and the tip is calculated using the extended Hückel theory (EHT). Importantly, EHT provides the correct bulk Si band gap (as compared to local density approximation⁷) and captures the surface and band structure effects accurately.^{4,24,25} We incorporate an isolated DB in a H:Si(001)-(2 × 1) symmetric dimer unit cell, composed of 64 Si atoms with 8 at the sur-

face, out of which 7 are passivated and 1 is unpassivated which has the dangling bond, as shown in the inset of Fig. 4 [visualized using GAUSSVIEW (Ref. 27)]. Additional surface relaxation due to the DB is small,²⁶ and hence ignored. We calculate the surface Green's function (g_s) recursively²⁸ and find that the DB gives rise to a near-midgap state in the Si band gap, similar to Ref. 26. We assume a constant g_s for the tip, similar to Ref. 5. However, Σ_{tip} is still energy dependent, since it is defined as $[(E+i0^+)S_1-H_1]g_s[(E+i0^+)S_1^\dagger-H_1^\dagger]$, where S_1 and H_1 are the overlap and Hamiltonian matrices between the tip and styrene molecule. For a good STS tip, which can give atomic resolution, the last tip atom at the apex dominates STS and, hence, we use a single tungsten (W) atom as tip. Transport quantities are then calculated through a single molecule. The molecular structure is taken from Ref. 5, which reports structure for a styrene molecule on hydrogenated Si surface. There is an important difference between the bonding geometries of styrene on hydrogenated and unpassivated Si. For hydrogenated Si, one C atom of styrene bonds to one Si atom, as shown in Fig. 1. For unpassivated Si, styrene goes through a cycloaddition process and the two C atoms on the styrene bind with two atoms of a Si dimer (not shown in this paper).

For Σ_{tip} , the EHT parameters of the s -orbital basis set are modified²⁹ (similar to Ref. 30) to get an appropriate apparent barrier height (ϕ_{ap}). We obtain $\phi_{ap}=4.3$ eV from the calculated $I(z)$ plot³¹ with 2 V applied at the tip, as shown in Fig. 2(a). This apparent barrier height is about 10 eV with the original parameters. Apart from this, the HOMO level of W atom lies at -10.73 eV, whereas the work function of W(110) tip is around 5.2 eV; therefore, we have an offset of 5.53 eV with respect to vacuum. Similarly, the Si conduction band edge (E_c) obtained from EHT has an offset of 7.75 eV. To calculate the offset of styrene, we use the HOMO level obtained from DFT-B3PW91/6-311g^{*} calculations³² as a reference, since the occupied states in density functional theory (DFT) are relatively well characterized.³³ To ensure a proper alignment with respect to vacuum, we shift the Hamiltonians by the above-mentioned offsets $E_{\text{offset}-i,j}$ for the systems i and j within the EHT procedure as follows:

$$H_{ij} = \frac{1}{2}S_{ij}(K_i H_{ii} + K_j H_{jj} + E_{\text{offset}-i} + E_{\text{offset}-j})$$

In order to match the experimentally observed onset voltages, we shift the molecular levels by +0.5 eV (shifted toward the valence band minimum). This shift is a one time adjustment for all the molecules under consideration and, hence, it affects the onset voltages of all the molecules by an offset of +0.5 V. Further changes in the onset voltages come due to the DB potential U_{DB} , which varies inversely with distance of different molecules from the DB. Since the density of states inside the HOMO–lowest unoccupied molecular orbital gap is quite small, a shift of 0.5 V can be caused by a very small change in the Hartree potential at equilibrium due to small charge transfer. However, the line shapes of the calculated I - V characteristics are not sensitive to this shift and they remain convex (see Sec. III). Incorporating this shift results in the HOMO level being about 0.4 eV be-

low the valence band edge (after incorporating the effect of Si contact as well in the form of Si self-energy, the real part of the self-energy shifts the molecular levels). This means that the HOMO level is about 0.9 eV below the valence band edge before applying this shift. The position of the HOMO level in our study is different from that in Ref. 3, where it is reported to be about 1 eV below the valence band edge. However, the difference in our case is that the styrene chain is in the vicinity of a charged dangling bond which could change the local nature of Si-C bond electrostatics. This governs the charge transfer at equilibrium, whereas in Ref. 3, there is no dangling bond. Furthermore, we do not calculate the charge transfer at equilibrium; rather, we use the shift in energy levels due to charge transfer as an adjusting parameter. In short, there are two fitting parameters in these calculations, shift of energy levels (a one time adjustment) and dephasing strength D . These two fitting parameters are used to capture two independent features in the experiment. The first one, i.e., shift of energy levels, is used to quantitatively match the experimentally observed onset voltages and it does not affect the line shapes observed whether we include dephasing or not. The second parameter, i.e., dephasing strength D , is used to reproduce the experimentally observed *concave* line shapes. The dephasing affects the onset voltage in a minor fashion since it broadens the energy levels and, hence, current starts flowing at lower tip voltages.

We solve the three-dimensional (3D) Laplace equation using the finite-element method to obtain the potential profile across styrene due to the tip voltage. This method has been discussed in detail in Ref. 17. This method also provides the zero bias band lineup potential due to the Fermi level mismatch of 1.15 eV between the tip and n^+ +Si. Solving for a 3D potential ensures that the Stark effect is captured for the applied tip voltage. Furthermore, for the experimental conditions, the molecular levels shift by about one-tenth of the applied tip voltage and/or Fermi level mismatch, since the tip is quite far from the styrene molecules. This scenario is different from the ones reported in Refs. 5 and 6, where the molecular levels shift by about one-third of the tip voltage because the tip is quite close to the molecule. Apart from this, the tip heights are modified³⁴ to reflect actual changes during experimental data acquisition³⁵ and, hence, tip heights are not used as adjustment parameters. Rather, it implies that our model is flexible to incorporate the very delicate experimental details.

For calculating the potential due to the DB, a 3D finite-element continuum calculation³⁶ is performed by taking into account the DB's approximate shape.³⁷ The styrene chain is approximated by a 100 Å long 3D box with width and height corresponding to those of styrene and having a relative dielectric constant of about 2.4. This box is placed on a Si bulk having a relative dielectric constant of about 12. A scanning tunneling microscopy (STM) tip is placed about 1 nm above the styrene chain in the form of a metallic sheet. An average of the calculated potential (U_{DB}) taken over the lateral cross section is included in our transport calculation. A plot of U_{DB} as a function of distance from the DB is shown in Fig. 2(b). The potential profile across a molecule 4 Å away from the DB [shown in the inset of Fig. 2(b)] shows a weak electrostatic contribution in Si. Incorporating U_{DB} in an averaged

fashion ignores the Stark effect within a single molecule due to charge on the dangling bond. This may quantitatively affect the results in a minor way because as seen in the inset of Fig. 2(b), the dangling bond potential is comparatively constant over a single molecule, i.e., within about 0.5–0.7 eV. This simple continuum model seems to be satisfactory for calculating the electrostatics of the DB because (1) the screening effect of the styrene chain should be small due to the one-dimensional nature of the styrene chain. In particular, occupied states are more localized than unoccupied states and, hence, this screening is expected to be small for occupied states (a case discussed in this paper). (2) We obtain a hyperbolic dependence as a function of distance from the dangling bond, i.e., $U_{DB} \approx 2.4 \text{ eV}/d \text{ \AA}$, which is expected. For calculating the electrostatic contribution, treating the charged DB, styrene chain, and n^{++} doped Si in an atomistic manner may result in a quantitatively different U_{DB} ; however, it is still expected to show a hyperbolic dependence and can be readily incorporated in our model. Such a change would result in different onset voltages as a function of distance from the dangling bond; however, the reported line shapes in Sec. III would remain the same.

Moreover, based on a finite-element MEDICI (Ref. 38) calculation, we conclude that tip induced band bending is also negligible. Additionally, dopants in n^+ Si introduce states approximately 50 meV (Ref. 39) below E_c , which contribute weakly⁴⁰ to transport for a tip voltage of about 50 meV. In our calculations, we ignore the above-mentioned effects. The Hartree potential for the molecule is included via the complete neglect of differential overlap method.⁴¹ Image effects are incorporated¹⁷ to ensure that self-consistency is not overestimated, which can alter results significantly. In all of the above electrostatic calculations, the tip is taken to be a metal sheet having a work function of 5.2 eV—a value attributed to W(110) tip.

III. DISCUSSION OF RESULTS

A transport calculation to study the effect of dephasing for a molecule 12 Å away from the DB is presented in Fig. 3(a). Without dephasing, the line shape [red (dark gray) dotted line] does not match with the experiment [blue (dark gray) × marks]. The line shapes for the theoretically calculated and experimentally observed I - V characteristics are quite different. The experimentally observed line shapes are concave, whereas the calculated line shape has a *convex* character. For coherent transport, obtaining a convex line shape is expected because it represents that current starts flowing through a level and then saturates when the level is fully inside the bias window. The corresponding conductance peak (not shown) has a full width of half maximum of about 0.2 eV. This is roughly equal to the coupling between styrene and Si contact because the tip is quite far and, hence, the I - V characteristics do not get affected much by the Hartree potential due to the nonequilibrium carrier statistics. This small coupling is expected since styrene binds with Si through only one Si-C bond and HOMO is localized on the aromatic ring of the styrene molecule, see, e.g., Refs. 9 and 44. However, after including dephasing (with $D=1.4 \text{ eV}^2$), not only is the line

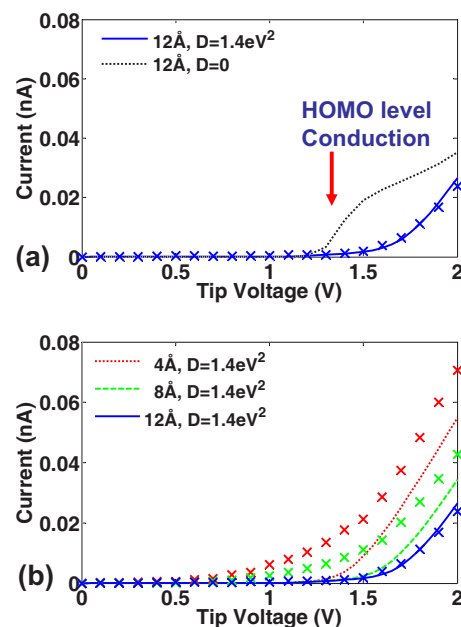


FIG. 3. (Color online) Effect of dephasing and electrostatic contribution of the DB on transport properties. (a) Calculated I - V plots for the molecule 12 Å away with and without dephasing. Without dephasing, the line shape [red (dark gray) dotted line] does not match with the experiment (blue × marks). With $D=1.4 \text{ eV}^2$, there is a good quantitative agreement with the experiment. (b) Calculated I - V plots for molecules 4, 8, and 12 Å away from the DB after incorporating U_{DB} .

shape reproduced, but good quantitative agreement with the experiment is achieved.

This transition from a convex line shape to concave line shape needs further discussion. The physical effect of dephasing is that it broadens the molecular levels. Since the LDOS of Si contact (see Fig. 4) increases with decreasing energy and/or increasing positive tip voltage, the current starts increasing in a fashion proportional to the coupling to the Si contact, which is proportional to the LDOS of Si contact. In this case, as can be seen in Fig. 4, the LDOS increases with decreasing energy as one goes away from the valence band edge. The current increases with increasing tip voltage in a concave manner because of this increase in LDOS of Si contact. This LDOS corresponds to increased

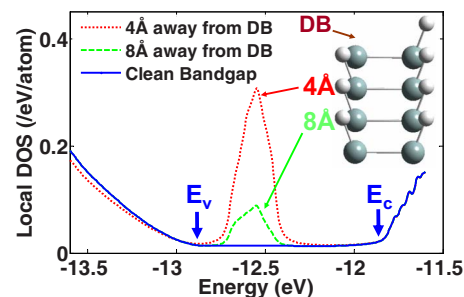


FIG. 4. (Color online) Electronic contribution of the DB. The calculated local density of states of Si atoms 4 and 8 Å from the DB shows that the DB introduces a near-midgap state. The inset shows the surface portion of the unit cell used.

surface Green's function of Si, and hence larger Si self-energy Σ_{Si} , which results in a higher current. In order to adjust for this, we have to use higher tip height of 8.67 Å in our model after including dephasing instead of 7.79 Å for coherent transport to get the same current level. Since, experimentally, tip heights in general remain to be unknown, this variation is acceptable. However, relative tip heights are known experimentally. In the set of experiments we consider, these relative heights were changed³⁵ during experimental data acquisition for the molecules 4 and 8 Å away from the DB and we include them in our model.³⁴

Using the same D for molecules 4 and 8 Å away from the DB and including U_{DB} , we obtain the I - V plots shown in Fig. 3(b). Although the line shapes are similar to the experimentally observed line shapes, there is still a significant mismatch in the onset voltages between experiment and calculation for molecules 4 and 8 Å away. Experimentally, their onset voltages are grouped together and are much smaller than the calculated ones. This is expected since the valence band edge corresponds to a tip voltage of about 1.2 V and, hence, very small current should be expected for tip voltages below 1.2 V. However, as can be seen in Fig. 3(b), experimentally, conduction starts from about 0.5 V. We interpret this disagreement between experiment and calculation to be induced by the DB. Besides contributing electrostatically, the DB introduces a near-midgap state in the LDOS of Si atoms beneath the styrene chain extending up to be about 10 Å. The calculated LDOS for Si atoms 4 and 8 Å away from the DB is shown in Fig. 4. A near-midgap state is clearly visible inside the band gap, which is responsible for the early onset of conduction at about 0.5 V of tip voltage. The LDOS contribution of the DB state exponentially decays and is nearly absent for a styrene molecule about 12 Å away.

In our transport model, the DB is taken to be fully occupied under equilibrium and nonequilibrium conditions through inelastic processes inside the Si contact. This is a valid assumption since the energetic location of the DB state is well below the chemical potential. Furthermore, the electronic structure calculations are for intrinsic Si, where the effect of dopants and charged DB is ignored for simplicity; otherwise, the calculations become computationally prohibitive. The effect of doping, however, is electrostatically included in our transport calculations by adjusting the equilibrium Si chemical potential. Besides this, treating the DB state as charged is expected to cause a shift in its energetic position within the band gap. Since these states are thermally broadened on the order of 0.5 eV or more⁴² at room temperature and that the DB state is close to midgap, the results presented are expected to be comparatively insensitive to this shift.

In Fig. 5(a), the bias dependent calculated transmission $T(E, V)$ through molecules 4, 8, and 12 Å away from the DB is shown. For molecules 4 and 8 Å away, there is finite conduction inside the band gap due to this DB state, which is absent for the molecule 12 Å away. For the molecule 4 Å away, at higher tip voltages, the level below the HOMO level, i.e., HOMO-1 level, also starts conducting. Figure 5(b) shows the corresponding I - V characteristics after including the DB's electronic and electrostatic contributions with $D = 1.4 \text{ eV}^2$. The onset voltages for molecules 4 and 8 Å away

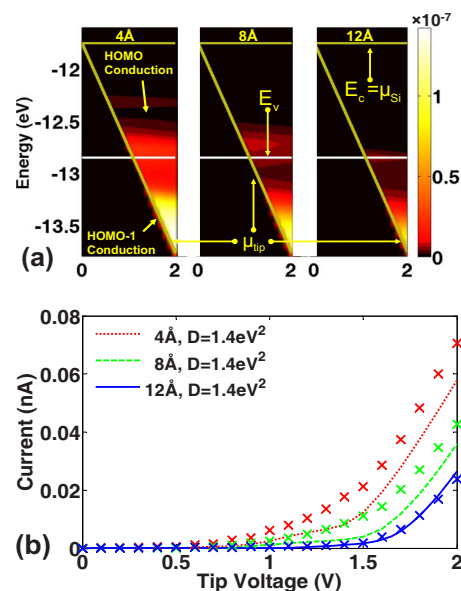


FIG. 5. (Color online) Effect of electronic and electrostatic contributions of the DB on transport properties. (a) $T(E, V)[f_{\text{tip}} - f_{\text{Si}}]$ plots [where $T(E, V)$ is the transmission and $f_{\text{tip}, \text{Si}}$ are the Fermi functions for the contacts] for molecules 4, 8, and 12 Å away from the DB. For molecules 4 and 8 Å away, there is conduction inside the band gap due to electronic contribution of the DB. (b) Corresponding I - V plots. Onset voltages for molecules 4 and 8 Å away match well with the experiment, whereas line shapes do not.

match reasonably well with the experiment and are grouped together, but the line shapes still differ. There is an increase in current at about 0.6 V and then current tends to saturate. This is because the contribution of the DB state is small in this energy range. Using a higher D of 1.85 eV^2 for molecules 4 and 8 Å away broadens the molecular spectral density more, and hence reproduces the experimentally observed line shapes, as shown in Fig. 1. These molecules, being at the end of the styrene chain, may have more phonon degrees of freedom, thus resulting in a higher dephasing. Another possible explanation could be that the dephasing processes inside the Si contact broaden the LDOS contribution of the midgap state. Further experimental and theoretical work needs to be carried out to establish a detailed understanding of the dephasing mechanism. For example, conducting temperature dependent transport experiments would sharpen the spectroscopic features with decreasing temperature since $D \propto T$ for $\hbar\omega \ll k_B T$. Apart from this, using different molecules with varying HOMO levels may give an insight into the electronic contribution.

Since we are calculating the transport properties of an isolated styrene molecule and comparing with the styrene molecules embedded in a chain, the question if we are missing something arises. As long as one can obtain atomic resolution with the tip, which means that there is one apex atom and the tip is above a styrene molecule, the conduction from the tip to other styrene molecules inside the chain is expected to be small. Because styrene molecules are about 4 Å away and if the tip is about 8 Å above the styrene molecule, the distance of the tip atom from the next styrene molecule would be about 9 Å. This should result in an order of mag-

nitude lower current through the next styrene molecule. Therefore, although the conduction along the styrene chain may be noticeable, as discussed in Ref. 3, since the tip is placed above a styrene molecule, the lowest conduction path is still through this particular styrene molecule and, hence, conduction through the neighboring styrene molecules would still be small. However, if the tip is placed between two styrene molecules (a case not discussed in this paper), one has to consider transport through both the styrene molecules and tunneling between them. Since, in our case, the neighboring styrene molecules are expected to remain in equilibrium, the effect of self-consistent potential variation in the neighboring styrene molecules can be ignored as well. It should be noted that our case is different from that of a self-assembled monolayer device contacted by a flat contact because, in this case, all the molecules are expected to conduct and, hence, a molecule would be affected by the self-consistent potential of the neighboring molecules. The self-consistent potential of the styrene molecule through which the conduction is occurring could affect the neighboring styrene molecule electrostatics and, in return, the perturbed neighboring molecules could affect the self-consistent potential of the conducting molecule itself. Since the tip is far from the molecule and self-consistent potential is small (although not negligible), this effect is expected to be small.

We also ignore the tilt angle of the styrene molecule with respect to the Si substrate as a function of distance from the dangling bond that may be present in reality. It has been shown previously that the tilt angle for a styrene chain in the absence of the dangling bond as a function of distance from the end of the styrene chain may lead to significant changes in the current flowing through the styrene chain, and hence the observed STM images. This end effect has been observed experimentally for low bias and qualitatively reproduced theoretically in Ref. 3. This end effect vanishes at higher bias and is still not well understood. As shown experimentally in Ref. 9, in the presence of a charged dangling bond at the end of the styrene chain, this end effect is not present. Therefore, assuming that the tilt angle of the molecules near the end of the chain does not change seems to be a good approximation. However, a detailed quantitative study is needed. It would also be interesting to analyze how the low lying phonon spectrum gets modified for a styrene chain on Si surface in the presence of a dangling bond, whereas, previously, the phonon spectrum of a single molecule on a substrate has been discussed.^{11,12} The intermolecular interactions are expected to give rise to new peaks in the phonon spectrum.

Apart from this, there is a possibility that the neighboring styrene molecules may be electronically affecting each other. Although the styrene molecules are not chemically bonded, there may still be some effect of broadening. In particular, this effect has been theoretically addressed in Ref. 3, where it was concluded that it would be higher for unoccupied states than for occupied states. This conclusion is consistent with that in Ref. 43, where, based on DFT calculations, it has been reported that for occupied states, up to 80% of the wave function is localized on the aromatic ring of the styrene molecule. Furthermore, the unoccupied states are also analyzed theoretically in Refs. 44 and 45, reaching the same conclusion. This means that hybridization along the chain for occu-

ried state is small and, hence, broadening caused by it is expected to be small. Another calculation in Ref. 9 shows similar behavior with additional information that for the energy range corresponding to tip voltages less than about +2 V (the voltage range discussed in this paper), the coupling between the styrene molecules is small and, hence, the experimental observation of the slope effect was attributed to this localized charge on styrene molecules in this voltage range. However, for larger energy range and for tip voltages greater than about +2 V (a case not discussed in this paper), the spectral densities on neighboring styrene molecules start overlapping and charge density becomes delocalized and, hence, slope effect vanishes. Since, in our study, we are calculating transport properties for occupied states in the 0–2 V tip voltage range, this effect is expected to be small in our voltage range of interest, and hence is not included in our calculations.

IV. CONCLUSIONS

We have examined occupied level conduction through a styrene molecule in the vicinity of a negatively charged DB on a n^{++} H:Si(001)-(2×1) surface. We put forward that the DB does affect conduction through styrene not only electrostatically within approximately 100 Å but also electronically up to 10 Å from the DB by introducing a near-midgap state in the LDOS of neighboring Si atoms. Dephasing is further expected to play a significant role in these experiments.

ACKNOWLEDGMENTS

We acknowledge fruitful discussions with S. Datta, P. G. Piva, and R. A. Wolkow and thank the latter two for sharing their experimental data in electronic format. We acknowledge F. Zahid and T. Raza for the HUCKEL-IV 3.0 (Ref. 17) codes. This work was supported by the NASA Institute for Nanoelectronics and Computing and ARO-DURINT. Computational facilities were provided by the NSF Network for Computational Nanotechnology. We also thank E. C. Kan, A. W. Ghosh, and G.-C. Liang for useful discussions.

APPENDIX

In this section, we show the derivation of Eq. (2). The scattering inflow function (Σ_s^{in}), outflow function (Σ_s^{out}), and broadening function (Γ_s) are defined as:^{19,20}

$$\begin{aligned} \Sigma_s^{in,out}(E) &= \int_0^\infty \frac{d(\hbar\omega)}{2\pi} D^{em,ab}(\hbar\omega) S G^{n,p}(E + \hbar\omega) S \\ &\quad + D^{ab,em}(\hbar\omega) S G^{n,p}(E - \hbar\omega) S, \end{aligned}$$

$$\begin{aligned} \Gamma_s(E) &= \Sigma_s^{in} + \Sigma_s^{out} \\ &= \int_0^\infty \frac{d(\hbar\omega)}{2\pi} D^{em}(\hbar\omega) S [G^n(E + \hbar\omega) + G^p(E - \hbar\omega)] S \\ &\quad + D^{ab}(\hbar\omega) S [G^n(E - \hbar\omega) + G^p(E + \hbar\omega)] S, \end{aligned}$$

where $D^{em}(\hbar\omega) = (N+1)D_o(\hbar\omega)$ and $D^{ab}(\hbar\omega) = ND_o(\hbar\omega)$ are

emission and absorption dephasing functions, respectively, and are related by $D^{ab}/D^{em} = \exp(-\hbar\omega/k_B T)$. N is the equilibrium number of phonons given by Bose-Einstein statistics as $1/[\exp(\hbar\omega/k_B T) - 1]$. For $\hbar\omega \ll k_B T$, $N + 1 \approx N \approx k_B T / \hbar\omega$ by keeping the first term in the Taylor series expansion of $\exp(\hbar\omega/k_B T) \approx 1 + \hbar\omega/k_B T$, which leads to

$$\Gamma_s(E) = \int_0^\infty \frac{d(\hbar\omega)}{2\pi} [D^{em}(\hbar\omega) + D^{ab}(\hbar\omega)] SA(E)S$$

and

$$D^{em}(\hbar\omega) \approx D^{ab}(\hbar\omega) = ND_o(\hbar\omega) \approx \frac{k_B T}{\hbar\omega} D_o(\hbar\omega).$$

Substituting these results in the above Equation gives Eq. (2):

$$\Gamma_s(E) \approx T \underbrace{\int_0^\infty \frac{d(\hbar\omega)}{2\pi} \frac{2k_B D_o(\hbar\omega)}{\hbar\omega}}_D SA(E)S.$$

The presence of low lying phonon modes depends on many details (type of molecule, surface, bias voltage, etc.). This implies that not only the energy ($\hbar\omega$) of the phonon modes would change under different conditions but also the associated dephasing functions D_o . We leave the detailed study of these phonon modes for the styrene chain on Si surface in the presence of a dangling bond for future work and in this study treat this effect in an average manner by using the dephasing strength D as an adjusting parameter.

-
- ¹R. J. Hamers, R. M. Tromp, and J. E. Demuth, Phys. Rev. B **34**, 5343 (1986).
- ²R. Wolkow and Ph. Avouris, Phys. Rev. Lett. **60**, 1049 (1988).
- ³G. Kirczenow, P. G. Piva, and R. A. Wolkow, Phys. Rev. B **72**, 245306 (2005).
- ⁴G.-C. Liang and A. W. Ghosh, Phys. Rev. Lett. **95**, 076403 (2005) and references therein; G. Comtet and G. Dujardin, Science **308**, 1000 (2005).
- ⁵T. Rakshit, G.-C. Liang, A. W. Ghosh, and S. Datta, Nano Lett. **4**, 1803 (2004).
- ⁶N. P. Guisinger, N. L. Yolder, and M. C. Hersam, Proc. Natl. Acad. Sci. U.S.A. **102**, 8828 (2005).
- ⁷W. Lu, V. Meunier, and J. Bernholc, Phys. Rev. Lett. **95**, 206805 (2005).
- ⁸J. L. Pitters and R. A. Wolkow, Nano Lett. **6**, 390 (2006).
- ⁹P. G. Piva, G. A. DiLabio, J. L. Pitters, J. Zikovsky, M. Rezeq, S. Dogel, W. A. Hofer, and R. A. Wolkow, Nature (London) **435**, 658 (2005).
- ¹⁰P. G. Piva and R. A. Wolkow (private communication). Experimentally, there is an uncertainty of \pm half a dimer spacing to determine the DB center. Therefore, 4 and 8 Å curves are more like 4 ± 2 and 8 ± 2 Å.
- ¹¹N. Sergueev, D. Roubtsov, and H. Guo, Phys. Rev. Lett. **95**, 146803 (2005).
- ¹²Y.-C. Chen, M. Zwolak, and M. D. Ventra, Nano Lett. **5**, 621 (2005).
- ¹³J. G. Kushmerick, J. Lazorcik, C. H. Patterson, R. Shashidhar, D. S. Seferosand, and G. C. Bazan, Nano Lett. **4**, 639 (2004).
- ¹⁴H. S. Kato, J. Noh, M. Hara, and M. Kawai, J. Phys. Chem. B **106**, 9655 (2002).
- ¹⁵H. Park, J. Park, A. K. L. Lim, E. H. Anderson, A. P. Alivisatos, and P. L. McEuen, Nature (London) **407**, 57 (2000).
- ¹⁶A. Devos and M. Lannoo, Phys. Rev. B **58**, 8236 (1998).
- ¹⁷F. Zahid, M. Paulsson, E. Polizzi, A. W. Ghosh, L. Siddiqui, and S. Datta, J. Chem. Phys. **123**, 064707 (2005).
- ¹⁸S. Datta, *Quantum Transport: Atom to Transistor* (Cambridge University Press, Cambridge, UK, 2005).
- ¹⁹G. D. Mahan, Phys. Rep. **145**, 251 (1987).
- ²⁰F. Zahid, M. Paulsson, and S. Datta, in *Advanced Semiconductors and Organic Nano-techniques III*, edited by H. Morkoc (Academic, San Diego, CA, 2003).
- ²¹M. Paulsson, T. Frederiksen, and M. Brandbyge, Nano Lett. **6**, 258 (2006).
- ²²J. Cerda and F. Soria, Phys. Rev. B **61**, 7965 (2000).
- ²³J. Howell, A. Rossi, D. Wallace, K. Haraki, and R. Hoffman, FORTICON8, QCPE Program 545, Department of Chemistry, Cornell University, Ithaca, NY 14853.
- ²⁴D. Kienle, K. H. Bevan, G.-C. Liang, L. Siddiqui, J. I. Cerda, and A. W. Ghosh, J. Appl. Phys. **100**, 043715 (2006).
- ²⁵H. Raza, Phys. Rev. B **76**, 045308 (2007).
- ²⁶S. Watanabe, Y. A. Ono, T. Hashizume, and Y. Wada, Phys. Rev. B **54**, R17308 (1996).
- ²⁷R. Dennington II, T. Keith, J. Millam, K. Eppinnett, W. L. Hovell, and R. Gilliland, GAUSSVIEW, Version 3.0, Semichem, Inc., Shawnee Mission, KS, 2003.
- ²⁸M. P. L. Sancho, J. M. L. Sancho, and J. Rubio, J. Phys. F: Met. Phys. **14**, 1205 (1984).
- ²⁹Original $\zeta=2.341$; modified $\zeta=1.104$ 27.
- ³⁰J. Cerda, A. Yoon, M. A. VanHove, P. Sautet, M. Salmeron, and G. A. Somorjai, Phys. Rev. B **56**, 15900 (1997).
- ³¹L. Olesen, M. Brandbyge, M. R. Sorensen, K. W. Jacobsen, E. Laegsgaard, I. Stensgaard, and F. Besenbacher, Phys. Rev. Lett. **76**, 1485 (1996).
- ³²M. J. Frisch *et al.*, GAUSSIAN 03, Revision B.03, Gaussian, Inc., Wallingford, CT, 2004.
- ³³R. M. Martin, *Electronic Structure: Basic Theory and Practical Methods* (Cambridge University Press, Cambridge, UK, 2004).
- ³⁴8.79, 8.73, and 8.67 Å for molecules 4, 8, and 12 Å away, respectively, unless otherwise stated.

- ³⁵P. G. Piva and R. A. Wolkow (private communication). During the constant current STM (not shown), the height profile of the styrene chain decreased $1.2 \pm 0.4 \text{ \AA}$ across its 60 \AA length. As this constant current height contour (with the current feedback loop 'ON') determined the starting tip-sample separation prior to acquiring individual I - V curves (with current feedback loop 'OFF'), I - V curves shown in Fig. 1, 3, and 5 in the present work and in Fig. 5(a) in Ref. 9 were acquired with decreasing tip-sample separation as the distance from the DB increased.
- ³⁶COMSOL is a trademark of COMSOL AB (comsol.com).
- ³⁷DB is approximated by a prolate spheroid with polar and equatorial radii given by 1.5 and 1 \AA , respectively, estimated with a B3PW91/6-311g* calculation. The relative dielectric constant for the dangling bond is taken as 1.
- ³⁸TMA MEDICI, two-dimensional device simulation program, Version 4.0, user's manual, Technology Modeling Associates, Inc., Sunnyvale, CA, 1997.
- ³⁹S. M. Sze, *Physics of Semiconductor Devices* (Wiley-Interscience, New York, 1981), Chap. 1.
- ⁴⁰R. M. Feenstra and J. A. Stroscio, *J. Vac. Sci. Technol. B* **5**, 923 (1987).
- ⁴¹J. A. Pople and G. A. Segal, *J. Chem. Phys.* **44**, 3289 (1966).
- ⁴²T. Hitosugi, T. Hashizume, S. Heike, Y. Wada, S. Watanabe, T. Hasegawa, and K. Kitazawa, *Appl. Phys. A: Mater. Sci. Process.* **66**, S695 (1998).
- ⁴³W. A. Hofer, A. J. Fisher, G. P. Lopinski, and R. A. Wolkow, *Chem. Phys. Lett.* **365**, 129 (2002).
- ⁴⁴G. P. Lopinski, D. D. M. Wayner, and R. A. Wolkow, *Nature (London)* **406**, 48 (2000).
- ⁴⁵J.-H. Cho, D.-H. Oh, and L. Kleinman, *Phys. Rev. B* **65**, 081310(R) (2002).